A Rao-Blackwellised Unscented Kalman Filtering for MPPT Estimation in Photovoltaic Systems

Tian Lan[1], Yan Zhang[2], Wanhong Zhang[2]

1. Department of Mechanical Engineering, Qinghai University, Qinghai 810016, P. R. China
E-mail: tianlan9308@gmail.com

2. Department of Chemical Machinery, Qinghai University, Qinghai 810016, P. R. China
E-mail: zy210825@163.com, zwh0511@163.com

Abstract: Maximum power point tracking (MPPT) technology suits photovoltaic (PV) systems analysis well. It has better improvement for power generation efficiency and control effectiveness. However, the inherent nonlinear characteristics of the photovoltaic system and external factors such as irradiance and temperature hinder the stable system operation at the maximum power point (MPP). In addition, the accuracy and complexity of the PV system modeling are crucial to the performance of the PV system. This paper develops a Rao-Blackwellised Unscented Kalman Filtering (RBUKF) method for MPPT. Specifically, We first apply the Lambert W function to represent the current as an explicit function of its voltage, avoiding the need for the iterative solution and thus achieving faster and more accurate execution. Then, to improve the performance of the Unscented Kalman Filter (UKF), the Rao-Blackwellised method is applied to dynamic systems with nonlinear equations of state and linear equations of measurement. The simulation results show that the proposed method outperforms the traditional UKF in different transient and steady-state cases.

Key Words: MPPT, UKF, Lambert W function, PV System, Rao-Blackwellised

1 Introduction

Among the various solar technologies available, the PV system is one of the most efficient and widely used due to its ability to convert sunlight directly into electrical energy. There are a number of factors that influence the power transfer efficiency of a PV system, including solar irradiance, panel temperature, as well as the electrical characteristics of the load. Therefore, it is critical to consider these factors when optimizing the design and operation of the system to achieve maximum power transfer efficiency and desired performance. However, the nonlinear characteristics of a PV system pose a significant challenge in achieving MPP extraction. One way to address this challenge is through the use of MPPT algorithms, which enable the PV system to constantly adjust its operating point to the MPP and improve its overall efficiency.

However, determining the best MPPT technique can be complex and time-consuming due to the differences in complexity, accuracy, convergence speed, cost, and efficiency associated with each method. Extensive literature describes and categorizes various MPPT techniques[1, 2]. These technologies maximize the power output of solar panels under different operating conditions. However, the nonlinear characteristics of PV arrays, coupled with the effects of temperature and irradiance on the power profile, pose significant challenges to traditional MPPT algorithms. Scholars have employed diverse AI methodologies, such as particle swarm optimization (PSO)[3], artificial neural networks (ANN)[4], fuzzy logic control (FLC) [5], and the Jaya algorithm (JAYA)[6], to overcome these constraints. Although optimization theory and high-speed processors have advanced, implementing intelligent MPPT algorithms can still be costly due to their dependence on multiple iterations

and high processing power.

The Extended Kalman Filter (EKF) is an efficient and widely-used method for nonlinear estimation due to its excellent performance in handling nonlinear systems. This method can be applied to various applications, including target tracking, mobile robot localization, and control of autonomous vehicles. The EKF relies on linearizing a nonlinear system model, which can produce inaccurate or unstable estimates when the system is involved in highly nonlinear problems. Compared with the EKF, the UKF provides improved state estimation for nonlinear systems. The UKF method avoids the need for linearization by using a set of carefully selected points (called sigma points) to approximate the mean and covariance of the state distribution. By propagating these sigma points through the nonlinear system model, the state estimates are updated based on the transformed mean and covariance of the distribution. In the case of highly nonlinear systems, the UKF has been demonstrated to be more accurate and efficient than the EKF[7, 8].

Although UKF has gained popularity in different fields, it is limited in analyzing PV array performance due to the implicit equation form of the PV equivalent circuit model. To overcome these challenges, we first introduce a novel five-parameter PV array model that employs a Lambert W function evaluation method and can more accurately predict the behavior of the array under various operating conditions, thus improving the efficiency of the MPPT strategy and enabling a more comprehensive analysis of the overall system performance. Second, to reduce the computational effort of the standard UKF algorithm, an RBUKF-based state estimator is proposed. According to simulations, the proposed RBUKF is superior to the UKF under different transient steady-state conditions.

The following is the organizational structure of this paper: Section II discusses the PV array model, including the Lambert W function, and presents the state space representations of the process and measurement models. Section III

describes the UKF standard algorithm and the RBUKF algorithm. Section IV shows the results of the simulation. Lastly, Section V concludes the paper.

2 Photovoltaic Array Modelling

2.1 Equivalent Circuit Model with Single Diode and Double Resistance

PV arrays are interconnected PV cells that must satisfy specific design requirements to function correctly. In order to accurately predict the performance of PV arrays, PV modeling is essential. The five-parameter single-diode model is commonly used due to its balance of simplicity and accuracy [9]. Fig. 1 depicts the equivalent circuit for a PV cell.
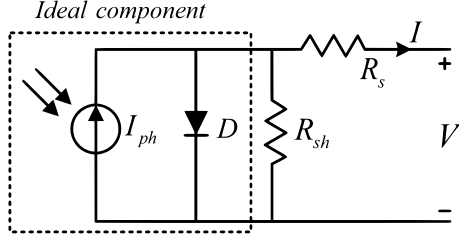

Fig. 1: Single-diode equivalent circuit models

The five parameters are photocurrent I_{ph}, diode saturation current I_s, diode modified ideality factor α, series resistance R_s, and parallel shunt resistance R_{sh}. This model can be adapted to work with different levels of PV systems, such as modules, panels, string modules, or entire arrays.

Incorporating resistive losses, the implicit expression for the current-voltage (I-V) of the analog circuit, following Kirchhoff's law, is:

$$I = I_{ph} - I_s(e^{\frac{V+IR_s}{\alpha}} - 1) - \frac{V+IR_s}{R_{sh}} \qquad (1)$$

2.2 Explicit Model Based on the Lambert W Function

The implicit character of equation (1) is apparent, which means that the corresponding output current I cannot be calculated directly for a given output voltage V. In order to address this issue, the Lambert W function has been proposed in the literature [10] as a means to reformulate the I-V equation for PV cells into an explicit form, as shown in equation (2). Equation (3) expresses the derivative of I with respect to V at the terminals of the panel. Thus, the differential conductance of the panel can be expressed as a function of its voltage V only using a nonlinear equation. This explicit representation improves accuracy, computational efficiency, and robustness. It avoids the challenges associated with numerical solution techniques, making it a viable option for various PV modeling and control applications.

$$I = \frac{R_{sh}(I_{ph} + I_s) - V}{R_s + R_{sh}}$$
$$- \frac{\alpha}{R_s} W \left\{ \frac{R_s R_{sh} I_s}{\alpha(R_s + R_{sh})} e^{\frac{R_s R_{sh}(I_{ph}+I_s)+R_{sh}V}{\alpha(R_s+R_{sh})}} \right\} \qquad (2)$$

$$\frac{dI}{dV} = -\frac{1}{(R_s + R_{sh})} - \frac{R_{sh}}{R_s(R_{sh} + R_s)}$$
$$W \left\{ \frac{R_s R_{sh} I_s}{\alpha(R_s + R_{sh})} e^{\frac{R_s R_{sh}(I_{ph}+I_s)+R_{sh}V}{\alpha(R_s+R_{sh})}} \right\} \qquad (3)$$

The I-V and P-V curves of the PV arrays were examined under standard test conditions (STC:$1000W/m^2$) and irradiance of $500W/m^2$, respectively. The results are displayed in Fig. 2. It can be seen that the Lambert W function method exhibits the same nonlinear characteristics as the actual solar panels within a reasonable range of parameters. Table.1 lists the five parameter values used to model the PV array for the STC (corresponding to the actual Sun-Power SPR-22-360 solar panel). These findings demonstrate the potential of the Lambert W function method as a reliable and efficient technique for PV modeling and control applications.
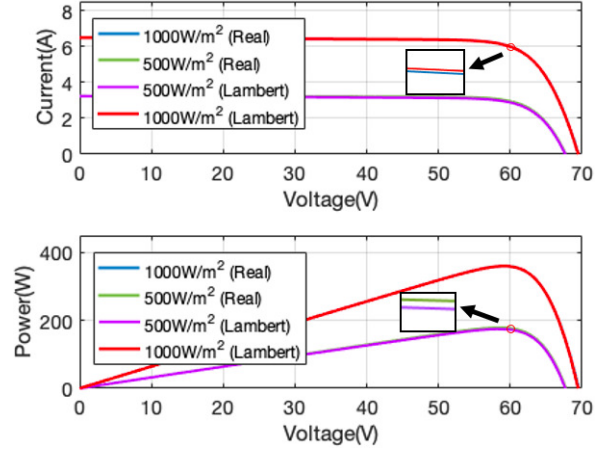

Fig. 2: I-V and P-V curves at different irradiance.

Table 1: Five Parameters of the PV Array (STC)

I_{ph}	I_s	α	R_s	R_{sh}
6.485	1.1444e-11	2.5702	492.4682	0.37591

2.3 The Lambert W Function

The Lambert function, denoted by $W(x)$, is a special function defined on the interval $-1/e \leq x < \infty$ for real variables x.

$$x = W(x)e^{W(x)} \qquad (4)$$

The Lambert function has a double value inside the brackets $[-1/e, 0]$. Furthermore, the Lambert function defines two different branches. $W_{-1}(x)$, for $W(x) \leq -1$, and $W_0(x)$, for $W(x) \geq -1$. Fig. 3 illustrates the different branches of the Lambert W function.
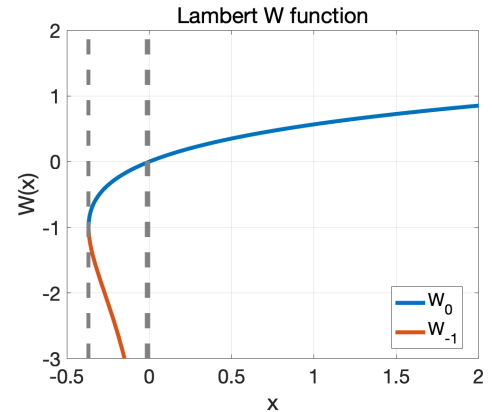

Fig. 3: The two main branches of the Lambert W function.

In PV applications, the parameter x is typically positive. Therefore, the Lambert function is restricted to the main branch, denoted by $W\{x\}$. Notably, the Lambert function cannot be represented by other elementary functions that can be calculated precisely or through approximate formulas. For this reason, various approximation methods have been proposed in the literature to compute this function accurately[11]. In this paper, we utilize an approximation method of similar nature as proposed by Barry et al.

$$W\{x\} = (1+\varepsilon)ln\left\{\frac{\frac{6}{5}x}{ln\left[\frac{\frac{12}{5}x}{ln(1+\frac{12}{5}x)}\right]}\right\} - \varepsilon ln\left[\frac{2x}{ln(1+2x)}\right]$$

$$(5)$$

where $\varepsilon = 0.4586887$ is a constant. The expression (5) is an exact approximation of $W_0(x) \geq 0$ with a maximum relative error of 0.196%.

2.4 Process Model & Measurement Model

Power-voltage (P-V) curves of PV arrays have a distinctive characteristic - the slope transitions from positive to negative as the operating point moves away from the MPP, as shown in Fig. 2. The MPPT algorithm uses this property to optimize the operating point to achieve maximum power output. We can obtain the discretized state space model as follows.

$$V_k = V_{k-1} + M\frac{dP}{dV} + w_{k-1} \tag{6}$$

$$Z_k = V_k + v_k \tag{7}$$

where M is the step-size corrector. We employ the instantaneous slope of the P-V curve, also known as dP/dV, to achieve a precise filter response. where $dP/dV = I + V(dI/dV)$. In order to enhance the integrity of the system simulation, the process and measurement equations are subjected to additive Gaussian random variables denoted as "w_k" and "v_k", with covariance matrices Q and R, respectively. This approach ensures that the simulation results closely align with real-world observations by introducing an element of disturbance to the equations.

3 Algorithm Descriptions

3.1 Unscented Kalman Filtering (UKF)

UKF is a method to estimate the state of nonlinear systems using a probabilistic framework. The UKF method differs from the traditional linearization of a nonlinear system by extracting sigma points from the state probability distribution and propagating them through the actual nonlinear system. This propagation allows for the computation of the statistical characteristics of the posterior distribution, which are then utilized for parameterization.

The UKF method achieves superior computational accuracy and stability in nonlinear distribution statistics, thus eliminating the derivation of Jacobian matrices and avoiding inaccuracies that arise from linearization errors due to neglect of higher-order terms. In order to elucidate the function of UKF, consider the following generic nonlinear state and measurement model:

$$\begin{cases} x_k = f(x_{k-1}) + w_{k-1} \\ z_k = h(x_k) + v_k \end{cases} \tag{8}$$

The steps for the UKF algorithm for model (8) are provided below:

3.1.1 Initialization

$$\hat{x}_0 = E[x_0] \tag{9}$$

$$P_0 = E[(x_0 - \hat{x}_0)(x_0 - \hat{x}_0)^T] \tag{10}$$

3.1.2 Compute the Sigma Points & Weights

Unscented Transformation(UT) is a technique for propagating the statistical characteristics of a random variable through a nonlinear transformation. Suppose we have a random variable x with mean $\bar{x}$ and covariance P. Compute the set of $2n + 1$ Sigma points $\mathcal{X}_i$, where $i = 0, 1, ..., 2n$, as follows:

$$\begin{cases} \mathcal{X}_0 = \bar{x}, \\ \mathcal{X}_i = \bar{x} + (\sqrt{(n+\lambda)P})_i, i = 1 \sim n \\ \mathcal{X}_i = \bar{x} - (\sqrt{(n+\lambda)P})_i, i = n+1 \sim 2n \end{cases} \tag{11}$$

UKF calculates the posterior mean and covariance by using the transformed sigma points and two sets of weighting factors (mean weighting and covariance weighting) with weighs ω_i given by

$$\begin{cases} \omega_0^{(m)} = \lambda/(n+\lambda) \\ \omega_0^{(c)} = \lambda/(n+\lambda) + (1 - \alpha^2 + \beta) \\ \omega_i^{(m)} = \omega_i^{(c)} = 1/[2(n+\lambda)] \qquad i = 1,...2n. \end{cases} \tag{12}$$

where n represents the dimensionality of the state vector estimated. the $\lambda = \alpha^2(n+\kappa) - n$ is a scaling parameter. The positive scaling constants α, κ, and β are critical to generating sigma points and the associated weights. α determines the spread of sigma points around the mean and is usually set to a small positive value, *i.e.*, $10^{-4} \leq \alpha \leq 1$. κ minimizes the higher-order errors associated with means and covariances. As a general rule, this takes a value equal to either $3 - n$ or 0. Finally, The parameter β is utilized to incorporate prior knowledge of the distribution. The optimal choice for β in the case of a Gaussian random variable is 2.

3.1.3 Time Update

For each iteration at instant k, Obtaining the transformed sigma points requires propagating the a-priori sigma points through a nonlinear process model. Based on the transformed sigma points, compute the weighted mean and covariance as follows:

$$\mathcal{X}_{i,k|k-1} = f(\mathcal{X}_{i,k-1|k-1}) \tag{13}$$

$$\hat{x}_{k|k-1} = \sum_{i=0}^{2n} \omega_i^{(m)} \mathcal{X}_{i,k|k-1} \tag{14}$$

$$P_{k|k-1} = \sum_{i=0}^{2n} \omega_i^{(c)} (\mathcal{X}_{i,k|k-1} - \hat{x}_{k|k-1}) \\ \times (\mathcal{X}_{i,k|k-1} - \hat{x}_{k|k-1})^T + Q \tag{15}$$

With the current best guess of the mean and covariance, the UT transformation is used again to generate new sigma points.

$$\begin{cases} \Psi_{0,k|k-1} = \hat{x}_{k|k-1}, \\ \Psi_{i,k|k-1} = \hat{x}_{k|k-1} + (\sqrt{(n+\lambda)P_{k|k-1}})_i, i = 1 \sim n \\ \Psi_{i,k|k-1} = \hat{x}_{k|k-1} - (\sqrt{(n+\lambda)P_{k|k-1}})_i, i = n+1 \sim 2n \end{cases}$$
$$(16)$$

By propagating the newly calculated sigma points through the nonlinear measurement model, the transformed sigma points in the measurement space are obtained, and they are used to calculate the predicted measurements and its covariances, as well as the cross-covariance between the predicted state and measurements.

$$Z_{i,k|k-1} = h(\Psi_{i,k|k-1}) \tag{17}$$

$$\hat{z}_{k|k-1} = \sum_{i=0}^{2n} \omega_i^{(m)} Z_{i,k|k-1} \tag{18}$$

$$P_{zz,k|k-1} = \sum_{i=0}^{2n} \omega_i^{(c)} (Z_{i,k|k-1} - \hat{z}_{k|k-1}) \\ \times (Z_{i,k|k-1} - \hat{z}_{k|k-1})^T + R \tag{19}$$

$$P_{xz,k|k-1} = \sum_{i=0}^{2n} \omega_i^{(c)} (\Psi_{i,k|k-1} - \hat{x}_{k|k-1}) \\ \times (Z_{i,k|k-1} - \hat{z}_{k|k-1})^T \tag{20}$$

3.1.4 Measurement Update

Calculate Kalman gain:

$$K_k = P_{xz,k|k-1} P_{zz,k|k-1}^{-1} \tag{21}$$

Finally, the state update and covariance update of the system are calculated.

$$\hat{x}_{k|k} = \hat{x}_{k|k-1} + K_k(z_k - \hat{z}_{k|k-1}) \tag{22}$$

$$P_{k|k} = P_{k|k-1} - K_k P_{zz,k|k-1} K_k^T \tag{23}$$

Upon reviewing the preceding steps, it is discernible that the UKF estimates the probability density distribution of the nonlinear function by utilizing a set of deterministic samples to approximate the posterior probability density of the state. This approach circumvents the need to approximate the nonlinear function and obviates the requirement for the derivation of the Jacobian matrix. Furthermore, by considering the higher order terms, UKF effectively addresses the limitations of low estimation accuracy and poor stability often observed with the EKF.

3.2 Rao-Blackwellised Unscented Kalman Filtering (RBUKF)

In UKF, the number of sigma points is intrinsically related to the dimensionality of the state vector. Using more sigma points will lead to more accurate estimates, as it captures more information about the probability distribution of the system states. However, using more sigma points also imposes an impractical computational burden. Using too few sigma points can also lead to state estimates uncertainty.

Therefore, there is a trade-off between the number of sigma points used and the computational cost of the UKF. Suppose the same level of estimation accuracy can be achieved by using fewer but better-located sigma points. In that case, the computational cost can be reduced. Therefore, to reduce the computational burden of sigma points, researchers have proposed various techniques to reduce the number of sigma points[12–14].

The Rao-Blackwellied technique is frequently employed to reduce the dimensionality of the state space model by marginalizing some state variables. This technique is particularly useful in particle filtering, which helps lower the computational costs involved[15]. RBUKF uses traditional statistical schemes to solve nonlinear problems when calculating means and covariances and uses Kalman filter theory to deal with linear issues. Therefore, it is particularly well-suited for combined linear-nonlinear systems.

Here, we present an RBUKF-based approach for MPPT estimation that takes advantage of the linearity of the measurement model to reduce the sampling requirement of the UKF *i.e.* $h(x_k) = H_k x_k$, where H_k is the measurement matrix at step k. Therefore, we can effectively reduce the computational steps in the time updating section, specifically steps (16) to (20). This includes updating the sigma points and calculating the predicted measurements, its covariances, and cross-covariances.

According to the Kalman filter theory, steps (16) to (20) in the time update of UKF can be replaced by the following calculation.

$$\hat{z}_{k|k-1} = H_k \hat{x}_{k|k-1} \tag{24}$$

$$P_{zz,k|k-1} = H_k P_{k|k-1} H_k^T + R \tag{25}$$

$$P_{xz,k|k-1} = P_{k|k-1} H_k^T \tag{26}$$

Hence, the initialization stage of the UKF algorithm, along with (13)-(15) and (21)-(26), constitutes the complete RBUKF algorithm. It is noteworthy that sigma points are updated only once in each step. The algorithm employs the update mechanism of Kalman Filter to calculate $\hat{z}_{k|k-1}$, $P_{zz,k|k-1}$, and $P_{xz,k|k-1}$ without utilizing sigma points. In summary, the RBUKF algorithm uses the unscented transformation technique to solve the nonlinear problem of the model and applies the Kalman filter theory to solve the linear problem of the model, which effectively reduces the computational burden and improves the estimation accuracy.

4 Simulation Results

Given the comprehensive analysis presented in the preceding sections, we compared the RBUKF-based estimator using a MATLAB/Simulink model. All test comparisons were performed in an identical standard testing environment. In the simulation, we corrupted the state variables and the measurement model with additive Gaussian white noise with a standard deviation of $\sigma = 1 \times 10^{-2}$. The filtering algorithm requires prior knowledge of two uncertainty matrices, R and Q, which are set to σ^2 and 50σ, respectively. Various steady-state and transient processes were considered to assess the estimation performance of UKF and RBUKF.

Table 2: Comparison of Maximum Output Power (M.O.P) under Different UKF Algorithms

Irradiation (W/m^2)	M.O.P (W)	M.O.P (UKF) (W)	M.O.P (RBUKF) (W)	Relative Error (UKF) $(\%)$	Relative Error (RBUKF) $(\%)$
1000	359.91	358.68	358.80	0.34	0.30
800	287.42	285.03	285.22	0.83	0.77
600	214.59	209.25	210.79	2.55	1.80
500	178.12	170.42	172.98	4.51	2.84
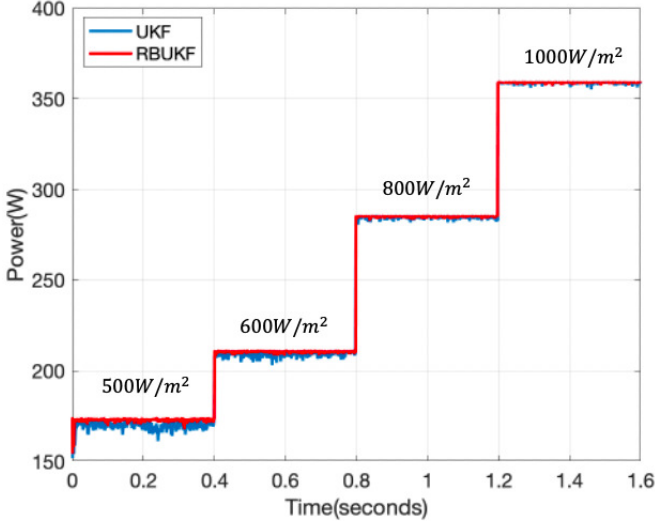
Fig. 4: Output power of UKF and RBUKF-based MPPT algorithms at $25°C$ constant temperature.

4.1 Efficiency of MPPT

The effectiveness of different UKF techniques for MPPT is an important area of research in the field of PV solar systems. The efficiency of MPPT is crucial to ensure that solar panels operate at their maximum power output, which may lead to increased energy production, improved system performance, and long-term cost savings. In this subsection, the performance of the PV system is evaluated by simulating and analyzing the ability to track the MPP under different irradiances. A constant temperature of $25°C$ is maintained throughout the test. The irradiation intensity is varied over a range of 500 W/m^2, 600 W/m^2, 800 W/m^2, and 1000 W/m^2 for 1.6 s. Fig. 4 illustrates the maximum power obtained under different irradiation conditions output.

Simulation results indicate that the conventional UKF and RBUKF algorithms demonstrate satisfactory tracking capability under standard test conditions. Nevertheless, under challenging operating conditions, such as varying solar irradiance levels ("50% shadow effect[16]"), the proposed RBUKF algorithm exhibits superior performance. To evaluate the effectiveness of MPPT, the values obtained in MPPT using the different UKF strategies mentioned above were compared with those provided by Matlab/Simulink for PV panels. The results are shown in Table.2.

4.2 Oscillation around the MPP

PV systems that can maintain a steady state with minimal oscillations around the MPP reduce energy losses and maximize the overall energy production of the system. Fig. 5 and Fig. 6 illustrate the local enlargements of the UKF and RBUKF algorithms in the steady-state region. As shown

in Fig. 5, the conventional UKF method has a large amplitude of oscillation with voltage at maximum power point (V_{MPP}) errors within (-2.12V, +2.12V). Moreover, the average PV output power oscillates by about ∓4.45W. According to Fig. 6, the proposed RBUKF algorithm reduces oscillation amplitudes, and the V_{MPP} error is within the range of (-1.32V, +1.32V). The oscillations around the MPP are lower, approximately ∓1.8 W. The proposed RBUKF is proven effective against the disturbance of system errors and has a better tracking performance. Table.3 summarizes the amount of oscillations around MPP and V_{MPP} for each UKF algorithm.
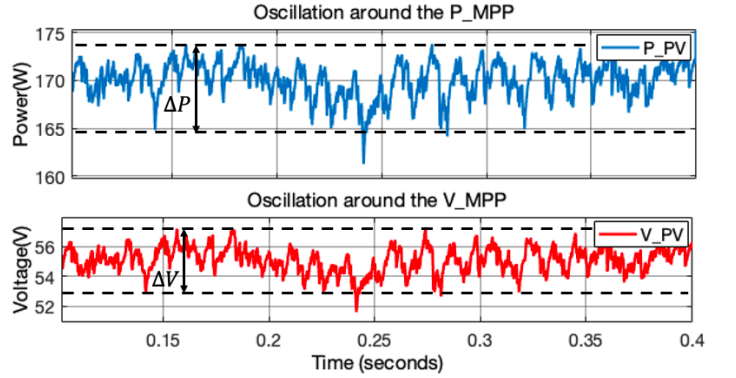

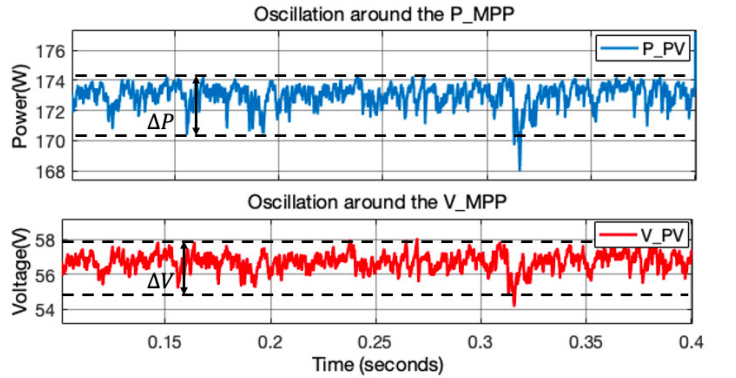Fig. 5: Oscillation around the MPP using UKF algorithm.

Fig. 6: Oscillation around the MPP using RBUKF algorithm.

Table 3: Oscillation Around the MPP

MPPT	UKF ($\%$)	RBUKF ($\%$)
ΔP	2.64	1.04
ΔV	3.86	2.34

5 Conclusion

This paper proposes the RBUKF algorithm applied to MPPT for PV systems. RBUKF directly utilizes the linear

part of the system equation, effectively reducing the computational load. Compared with the standard UKF, the RBUKF algorithm is more accurate and adapts to more complex situations. We also use the explicit PV model with the Lambert W function, providing a more accurate and robust implementation for optimizing PV system efficiency. It can be seen from the simulations that RBUKF has a significantly higher efficiency and superior performance compared to the standard UKF due to the reduction of a large amount of computational work.

References

[1] B. Yang, T. Zhu, J. Wang, H. Shu, T. Yu, X. Zhang, W. Yao, and L. Sun, "Comprehensive overview of maximum power point tracking algorithms of PV systems under partial shading condition," *Journal of Cleaner Production*, p. 121983, 2020.

[2] M. Sarvi and A. Azadian, "A comprehensive review and classified comparison of MPPT algorithms in PV systems," *Energy Systems*, vol. 13, no. 2, pp. 281–320, May 2022.

[3] S. Obukhov, A. Ibrahim, A. A. Zaki Diab, A. S. Al-Sumaiti, and R. Aboelsaud, "Optimal performance of dynamic particle swarm optimization based maximum power trackers for stand-alone PV system under partial shading conditions," *IEEE Access*, vol. 8, pp. 20770–20785, 2020.

[4] R. B. Roy, M. Rokonuzzaman, N. Amin, M. K. Mishu, S. Alahakoon, S. Rahman, N. Mithulananthan, K. S. Rahman, M. Shakeri, and J. Pasupuleti, "A comparative performance analysis of ANN algorithms for MPPT energy harvesting in solar PV system," *IEEE Access*, vol. 9, pp. 102137–102152, 2021.

[5] H. Rezk, M. Aly, M. Al-Dhaifallah, and M. Shoyama, "Design and hardware implementation of new adaptive fuzzy logic-based mppt control method for photovoltaic applications," *IEEE Access*, vol. 7, pp. 106427– 106438, Aug. 2019.

[6] C. Huang, Z. Zhang, L. Wang, Z. Song and H. Long, "A novel global maximum power point tracking method for PV system using Jaya algorithm," *2017 IEEE Conference on Energy Internet and Energy System Integration (EI2)*, Beijing, 2017, pp. 1-5.

[7] H. Khazraj, F. Faria da Silva, and C. L. Bak, "A performance comparison between extended kalman filter and unscented kalman filter in power system dynamic state estimation," in *2016 51st International Universities Power Engineering Conference (UPEC)*, Sep. 2016, pp. 1–6.

[8] I. Jokić, Ž. Zečević and B. Krstajić, "State-of-charge estimation of lithium-ion batteries using extended Kalman filter and unscented Kalman filter," *2018 23rd International Scientific-Professional Conference on Information Technology (IT)*, Zabljak, Montenegro, 2018, pp. 1-4.

[9] V. Stornelli, M. Muttillo, T. de Rubeis, and I. Nardi, "A new simplified five-parameter estimation method for single-diode model of photovoltaic panels," *Energies*, vol. 12, no. 22, p. 4271, Nov. 2019.

[10] E. Roibás-Millán et al., "Lambert W-function simplified expressions for photovoltaic current-voltage modelling," in *Proc. 20th IEEE Int. Conf. Environ. Elect. Eng.*, 2020, pp. 1630–1635.

[11] E. I. Batzelis, G. Anagnostou, C. Chakraborty, and B. C. Pal, "Computation of the Lambert W function in photovoltaic modeling," *Lect. Notes Elect. Eng.*, vol. 604, pp. 583–595, 2020.

[12] J. Kuti, I. J. Rudas, H. Gao, and P. Galambos, "Computationally relaxed unscented kalman filter," *IEEE Transactions on Cybernetics*, pp. 1–9, 2022.

[13] S. J. Julier and J. K. Uhlmann, "Reduced sigma point filters for the propagation of means and covariances through nonlinear transformations," in *Proc.American Control Conf.*, Anchorage, USA, 2002, pp. 887–892.

[14] Papakonstantinou, Konstantinos G., Mariyam Amir, and Gordon P. Warn. "A Scaled Spherical Simplex Filter (S3F) with a decreased n+2 sigma points set size and equivalent 2n+1 Unscented Kalman Filter (UKF) accuracy." *Mechanical Systems and Signal Processing* 163 (2022): 107433.

[15] A. K. Mishra, S. R. Shimjith and A. P. Tiwari, "Adaptive Unscented Kalman filtering for reactivity estimation in nuclear power plants," *IEEE Transactions on Nuclear Science*, vol. 66, no. 12, pp. 2388–2397, Dec 2019.

[16] F. Belhachat and C. Larbes, "Modeling, analysis and comparison of solar photovoltaic array configurations under partial shading conditions," *Sol. Energy*, vol. 120, pp. 399–418, 2015.